Results in Physics 8 (2018) 415–421

Contents lists available at ScienceDirect

Results in Physics

journal homepage: www.journals.elsevier.com/results-in-physics

Numerical study for melting heat transfer and homogeneous-heterogeneous reactions in flow involving carbon nanotubes

Tasawar Hayat [a,b], Khursheed Muhammad [a,*], Ahmed Alsaedi [b], Saleem Asghar [c]

[a] Department of Mathematics, Quaid-I-Azam University, 45320 Islamabad 44000, Pakistan
[b] Nonlinear Analysis and Applied Mathematics (NAAM) Research Group, Department of Mathematics, Faculty of Science, King Abdulaziz University, P.O. Box 80257, Jeddah 21589, Saudi Arabia
[c] Department of Mathematics, COMSATS Institute of Information and Technology, Islamabad 44000, Pakistan

ARTICLE INFO

Article history:
Received 1 November 2017
Received in revised form 25 November 2017
Accepted 12 December 2017
Available online 19 December 2017

Keywords:
Porous medium
Melting heat transfer
Carbon nanotubes
Homogeneous-heterogeneous reactions

ABSTRACT

Present work concentrates on melting heat transfer in three-dimensional flow of nanofluid over an impermeable stretchable surface. Analysis is made in presence of porous medium and homogeneous-heterogeneous reactions. Single and multi-wall CNTs (carbon nanotubes) are considered. Water is chosen as basefluid. Adequate transformations yield the non-linear ordinary differential systems. Solution of emerging problems is obtained using shooting method. Impacts of influential variables on velocity and temperature are discussed graphically. Skin friction coefficient and Nusselt number are numerically discussed. The results for MWCNTs and SWCNTs are compared and examined.

Introduction

It is noted that water, kerosine oil etc. are commonly used as base fluids for cooling purposes. Heat transfer rate in cooling process greatly depends on specific heat, density and thermal conductivity of the base fluid. One of the methods adopted for the enhancement of thermal conductivity of base fluid is through the addition of small sized particles. These small sized particles are known as nanoparticles. The homogenous mixture of the nanoparticles and basefluid is called nanofluid. Nanomaterials are made of oxide ceramics (Al_2o_3, Cuo etc.), carbide ceramics (SiC, TiC etc.), metal nitrides (AlN, SiN etc.), carbons (diamond, graphite, carbon nanotubes, fullerene etc.), functionalized nanomaterials and metals (Cu, Ag, Au etc.). Initially term Nano was utilized by Choi [1]. The shape of nanomaterials highly affects heat transport rate of fluids. Elias et al. [2] inspected the influence of shape of carbon nanomaterials on heat transfer rate. It is elaborated that tube shaped nanomaterials shows better performance for heat transfer coefficients, thermal conductivity and heat transfer rate. This is pursued by bricks, platelets, blades and spherical carbon nanomaterials respectively. Nanotubes are seamless cylindrical-shaped material of carbon with one or more layers of graphene. Carbon nanotubes with single graphene's layer are called single-wall carbon nanotubes while with more than one graphene's layer are called multi-wall carbon nanotubes. There are numerous applications of CNTs such as preparations of flat-panel displays, structural composite materials, antifouling paint, gas storage, radar-absorbing coating, micro and nanoelectronics, conductive plastics, technical textiles, batteries with improved lifetime, ultra-capacitors, extra strong fibers, biosensors for harmful gases etc. Due to the gamier chemical compatibility with biomolecules, the carbon nanotubes are used in biosensors and medical devices i.e. purification of drinking water, DNA and proteins [3]. MHD flow of nanomaterials with gyrotactic microorganism in a startified medium is examined by Waqas et al. [4]. Mixed convective entropy generation in a heated skewed enclosure of Cu-water nanofluid is numerically studied by Nayak et al. [5]. Hayat et al. [6] examined stagnation point flow of CNTs in presence of slip condition. Sheikholeslami and Ellahi [7] explored heat transfer in three dimensional flow of nanofluids with mesoscopic simulation of magnetic field. Hayat et al. [8] studied radiative flow of thixotropic nanofluid in presence of magnetohydrodynamics and Joule heating. Waqas et al. [9] explored radiative heat transfer in flow of Carreau nanofluid.

Melting and solidification are the most important phenomena in the technological processes. There is extensive range of applications of melting/freezing phenomenon of solid–liquid phase change materials. These include welding process, crystal growth, latent heat thermal energy storage, optimal utilization of energy, thermal protection, the freeze treatment of sewage, magma

* Corresponding author.
E-mail address: kmuhammd@math.qau.edu.pk (K. Muhammad).

https://doi.org/10.1016/j.rinp.2017.12.023
2211-3797/

solidification, preparation of semiconductors and thawing of frozan ground. Robert [10] initially described the melting by placing ice slab the stream of hot air. Melting effect in stagnation point flow of Maxwell fluid towards a surface with double-diffusive convection is inspected by Hayat et al. [11]. Melting heat transfer and radiation in MHD boundary layer flow is studied by Das [12]. Melting heat transfer in flow of micropolar fluid over a stretching/ shrinking surface is examined by Yacob et al. [13] in the region of stagnation point. Bachok et al. [14] explored heat melting transfer in stagnation point flow over a stretching/ shrinking surface. An experimental study on melting heat transfer by dispersing paraffin with Al_2O_3 nanoparticles is performed by Ho and Gao [15]. Few recent studies on stretchable surface can be further seen in the Refs. [16–23].

Homogeneous and heterogeneous reactions are the natural process of chemical reactions. Homogeneous reaction in fact occurs between the same phase (gases, liquids, solids) while heterogeneous reaction is two phase or different phase reaction (solid and gas, solid and liquid). Some of the chemical reactions are very slow or not at all in nature in the absence of a catalyst. Homogeneous and heterogeneous reactions have a complex interaction which involve the preparation and consumption of reactant species with different rate in the fluids as well on the surface of the catalyst such as the reaction occurs during the combustion. Homogeneous and heterogenous reactions during isothermal process in the boundary layer flow is explored by Merkin [24]. The flow and heat transfer of CNTs in the region of stagnation point with homogenous-reactions and Newton heating is inspected by Hayat et al. [25]. Kameswarn et al. [26] discussed the flow of nanofluid over porous stretching surface with homogeneous-heterogeneous reactions. Flow of micropolar fluid over a shrinking surface with homogeneous-heterogeneous reactions is studied by Shaw et al. [27]. The boundary layer flow towards a stretchable surface with homogeneous -heterogeneous reactions is considered by Bashok et al. [28]. Oscillatory behavior in homogeneous-heterogeneous reaction model is investigated by Song et al. [29]. Qayyum et al. [30] studied convective flow of third grade fluid over a variable thicked stretchable surface with chemical reactions. Homogenous-heterogeneous reactions in 3D flow with double diffusion is examined by Hayat et al. [31]. Tanveer et al. [32] elaborated homogeneous-heterogenous reactions in flow of Sisko fluid with mixed convection. Peristaltic flow with chemical reactions and Hall current is analyzed by Hayat et al. [33]. Khan et al. [34] explored homogeneous-heterogeneous reactions in stagnation point flow with Joule heating and viscous dissipation. Flow of nanofluid with chemical reactions over a stretchable variable thickness surface is analyzed by Hayat et al. [35]. Chemical reactions in stagnation point flow with non-Fourier heat flux is explored by Hayat et al. [36]. MHD flow with homogeneous-heterogenous reactions by a curved stretching surface is inspected by Imtiaz et al. [37]. MHD flow of an Oldroyd-B material with chemical reactions is studied by Hayat et al. [38]. Impact of homogeneous-heterogeneous reactions and non-Fourier heat flux towards a stretched surface is presented by Hayat et al. [39].

In order to enhance the thermophysical properties of heating or enlarging cooling rate the researchers and scientists have concentrated only on the dissolution of Ag, Al_2O_3, Cu nanomaterials in the base fluid. Here we have considered three dimensional flow with single-wall and multi-wall CNTs. Heat transfer by melting process is discussed. The emerging nonlinear system is solved by using shooting technique [41,42]. Both velocity and temperature are discussed graphically while skin friction coefficient and Nusselt are discussed numerically in view of influential variables.

Modeling

Consider three-dimensional flow of nanofluid over an impermeable stretchable surface. Fluid saturates the porous medium. Present flow subjected to melting heat and homogeneous-heterogeneous reactions is studied. CNTs are utilized in water. Moreover viscous dissipation and thermal radiation effect is neglected. Cartesian coordinates are chosen. Heat released during the reaction is also neglected.

The homogeneous reaction can be defined for cubic autocatalysis in the form:

$$A + 2B \to 3B, \qquad \text{rate} = k_1 ab^2, \tag{1}$$

while isothermal reaction of order first on the catalyst surface is:

$$A \to B, \qquad \text{rate} = k_s a. \tag{2}$$

Here a and b show concentration of chemical species A and B. The rate constants are represented by k_1 and k_s. These equations of reactions guarantee that the rate of reacton is zero in the external flow as well on the outer edge of boundary layer. After utilizing boundary layer approximations ($o(x) = o(y) = o(u) = o(v) = o(1)$, $o(w) = o(z) = o(\delta)$) one has

$$\frac{\partial u}{\partial x} + \frac{\partial v}{\partial y} + \frac{\partial w}{\partial z} = 0, \tag{3}$$

$$u\frac{\partial u}{\partial x} + v\frac{\partial u}{\partial y} + w\frac{\partial u}{\partial z} = \upsilon_{nf}\left(\frac{\partial^2 u}{\partial z^2} - \frac{u}{k_p}\right), \tag{4}$$

$$u\frac{\partial v}{\partial x} + v\frac{\partial v}{\partial y} + w\frac{\partial v}{\partial z} = \upsilon_{nf}\left(\frac{\partial^2 v}{\partial z^2} - \frac{v}{k_p}\right), \tag{5}$$

$$u\frac{\partial T}{\partial x} + v\frac{\partial T}{\partial y} + w\frac{\partial T}{\partial z} = \alpha_{nf}\frac{\partial^2 T}{\partial z^2}, \tag{6}$$

$$u\frac{\partial a}{\partial x} + v\frac{\partial a}{\partial y} + w\frac{\partial a}{\partial z} = D_A\frac{\partial^2 a}{\partial z^2} - k_1 ab^2, \tag{7}$$

$$u\frac{\partial b}{\partial x} + v\frac{\partial b}{\partial y} + w\frac{\partial b}{\partial z} = D_B\frac{\partial^2 b}{\partial z^2} + k_1 ab^2. \tag{8}$$

The boundary conditions are

$$\begin{aligned} &u = u_w(x) = mx, \quad v = v_w(y) = my, \quad D_A\left(\frac{\partial a}{\partial z}\right) = k_s a, \\ &D_B\left(\frac{\partial b}{\partial z}\right) = -k_s a \quad \text{at} \quad z = 0, \\ &u \to 0, \quad v \to 0, \quad T \to T_\infty \quad a \to a_0, \quad b0 \quad \text{when} \quad z \to \infty. \end{aligned} \tag{9}$$

In above expressions the velocity components are represented by u, v, and w in the x, y and z-direction respectively, υ_{nf} kinematic viscosity of nanofluids, α_{nf} thermal diffusivity of nanofluids, T and T_∞ fluid temperature and ambient temperature, D_A, D_B diffusion coefficient of species A and B, k_p the permeability while u_w and v_w the stretching velocities.

The condition related to melting heat transfer [10–15]:

$$k_{nf}\left(\frac{\partial T}{\partial z}\right)_{z=0} = \rho_{nf}[\lambda_1 + c_s(T_m - T_0)]w_{z=0}, \tag{10}$$

where ρ_{nf} is the density of nanofluid and λ_1 represents fluid's latent heat and c_s and T_0 the heat capacity and temperature of the solid surface respectively.

Xue [40] elaborated that earlier nanofluid models are only valid for rotational or spherical elliptical materials with very small axial ratio. On the basis of thermal conductivity space distribution the properties of carbon nanotubes cannot be described by these models. To overcome this void, a theoretical model on the base of Maxwell theory for elliptically rotational nanotubes having larger axial ratio and balancing the impacts of space distribution on carbon nanotubes is proposed by Xue [40].

Here

$$\mu_{nf}=\frac{\mu_f}{(1-\phi)^{2.5}},\qquad \upsilon_{nf}=\frac{\mu_{nf}}{\rho_{nf}},\qquad \rho_{nf}=(1-\phi)\rho_f+\phi\rho_{CNT},$$
$$\alpha_{nf}=\frac{k_{nf}}{\rho_{nf}(c_p)_{nf}},\qquad \frac{k_{nf}}{k_f}=\frac{(1-\phi)+2\phi\frac{k_{CNT}}{k_{CNT}-k_f}\ln\frac{k_{CNT}+k_f}{2k_f}}{(1-\phi)+2\phi\frac{kf}{k_{CNT}-k_f}\ln\frac{k_{CNT}+k_f}{2k_f}}, \tag{11}$$

where ϕ denotes the nanomaterial volume fraction, α_{nf} the thermal diffusivity, ρ_f the fluids density, k_{nf} and k_f the thermal conductivities of nanofluids and fluid while k_{CNT} the thermal conductivity of carbon nanotubes.

Transformations are taken as follows:

$$\begin{aligned}\eta &= z\sqrt{\tfrac{m}{\upsilon_f}}, \qquad u=mxF'(\eta), \qquad v=myG'(\eta),\\ w &= -\sqrt{m\upsilon_f}(F'(\eta)+G'(\eta)), \qquad \theta(\eta)=\tfrac{T-T_f}{T_\infty-T_f},\\ H(\eta) &= \tfrac{a}{a_0}, \qquad J(\eta)=\tfrac{b}{a_0}.\end{aligned} \tag{12}$$

Continuity Eq. (3) is satisfied automatically while laws of momentum conservation and energy give:

$$\left(\frac{1}{(1-\phi)^{2.5}\left(1-\phi+\phi\frac{\rho_{CNT}}{\rho_f}\right)}\right)F'''-\frac{\lambda}{(1-\phi)^{2.5}\left(1-\phi+\phi\frac{\rho_{CNT}}{\rho_f}\right)}F'-F'^2+(F+G)F''=0, \tag{13}$$

$$\left(\frac{1}{(1-\phi)^{2.5}\left(1-\phi+\phi\frac{\rho_{CNT}}{\rho_f}\right)}\right)G'''-\frac{\lambda}{(1-\phi)^{2.5}\left(1-\phi+\phi\frac{\rho_{CNT}}{\rho_f}\right)}G'-G'^2+(F+G)G''=0, \tag{14}$$

$$\left(\frac{k_{nf}/k_f}{\left(1-\phi+\phi\frac{(\rho c_p)_{CNT}}{(\rho c_p)_f}\right)}\right)\theta''+\Pr(F+G)\theta'=0, \tag{15}$$

$$\frac{1}{Sc}H''-K^*HJ^2+(F+G)H'=0, \tag{16}$$

$$\frac{\delta}{Sc}J''-K^*HJ^2+(F+G)J'=0, \tag{17}$$

with

$$\begin{aligned}&F'(0)=1,\quad G'(0)=1,\quad \frac{k_{nf}}{k_f}M\theta'(0)+\Pr\left(1-\phi+\phi\frac{\rho_{CNT}}{\rho_f}\right)(F(0)+G(0))=0,\\ &H'(0)=K_sH(0),\quad J'(0)=-\frac{K_s}{\delta}J(0),\\ &F'\to0,\quad G'\to0,\quad \theta\to1,\quad \text{as}\quad \eta\to\infty\end{aligned} \tag{18}$$

where λ shows the porosity parameter, Sc the Schmidt number, Pr the Prandtl number, K^* the strength of homogeneous parameter, K_s the strength of heterogeneous reaction parameter, M the melting parameter and δ the ratio of mass diffusion coefficients. These parameters are defined as follows:

$$\begin{aligned}&\lambda=\frac{\upsilon_f}{ak_p},\qquad Sc=\frac{\upsilon_f}{D_A},\qquad \Pr=\frac{\mu c_p}{k_f},\\ &K^*=\frac{a_0^2k_1x}{u_{w(x)}}=\frac{a_0^2k_1}{a},\qquad K_s=\frac{k_s}{D_A}\sqrt{\frac{\upsilon_f}{a}},\\ &M=\frac{c_p(T_\infty-T_m)}{\lambda_1+c_s(T_m-T_0)},\qquad \delta=\frac{D_B}{D_A}.\end{aligned} \tag{19}$$

Here we assume that D_A and D_B (Diffusion coefficients of species *A*and *B*) to be of comparable size. This statement further enables us to assume that both the diffusion coefficients D_A and D_B are equal for $\delta=1$. Hence [26]:

$$H(\eta)+J(\eta)=1. \tag{20}$$

From Eqs. (16) and (17) we have

$$\frac{1}{Sc}H''-K^*H(1-2H)^2+(F+G)H'=0, \tag{21}$$

The boundary conditions are

$$H'(0)=K_sH(0),\quad H(\eta)\to1\quad \text{as}\quad \eta\to\infty. \tag{22}$$

Dimensionless coefficient of skin friction and local Nusselt number are

$$\begin{aligned}C_f\mathrm{Re}_x^{1/2}&=\frac{1}{(1-\phi)^{2.5}}F''(0),\qquad C_f\mathrm{Re}_y^{1/2}\\ &=\frac{1}{(1-\phi)^{2.5}}G''(0),\qquad Nu_x\mathrm{Re}_x^{-1/2}=-\frac{k_{nf}}{k_f}\theta'(0),\end{aligned} \tag{23}$$

where $\mathrm{Re}_x=u_w(x+y)/v_f$ and $\mathrm{Re}_y=u_w(x+y)/v_f$ depicts the local Reynolds numbers.

Solutions

Built in routine of Mathematica for solving non-linear bvps via shooting method with an algorithm of fourth order Runge kutta is used to obtain the numerical solution of the systems consisting of Eqs. (13)–(15)and (21) and boundary conditions (17) and (22).

Discussion

Aim of this section is to interpret the impacts of influential variables on the velocity, temperature, skin friction coefficient and Nusselt number. Figs. (1) and (2) are sketched for the impacts of nanomaterial volume fraction on both axial and transverse

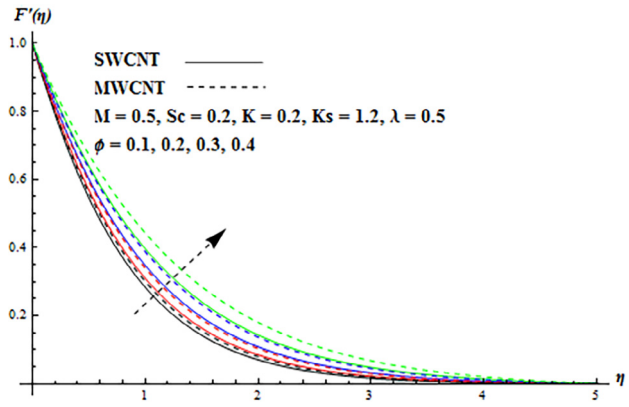

Fig. 1. ϕ variation for F'.

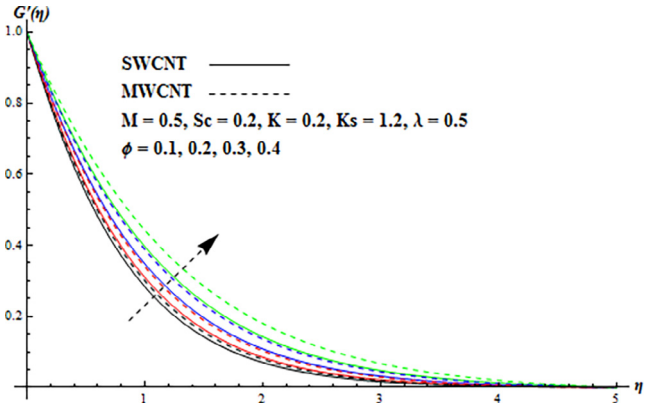

Fig. 2. ϕ variation for G'.

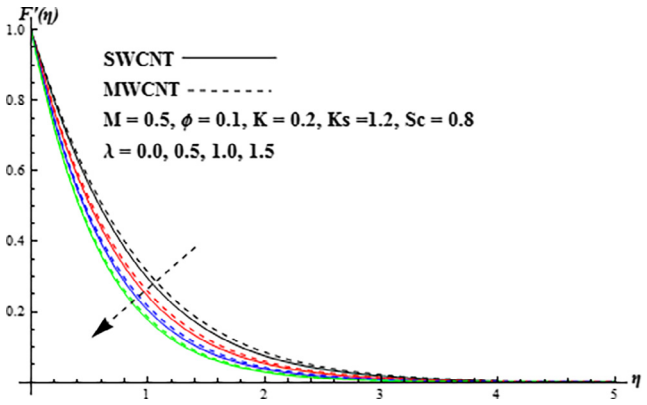

Fig. 3. λ variation for F'.

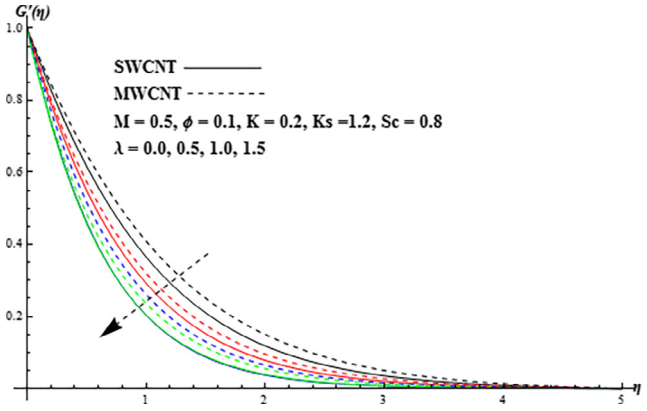

Fig. 4. λ variation for G'.

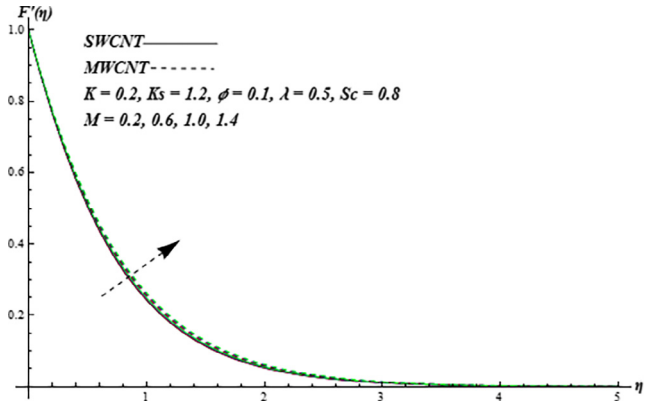

Fig. 5. M variation for F'.

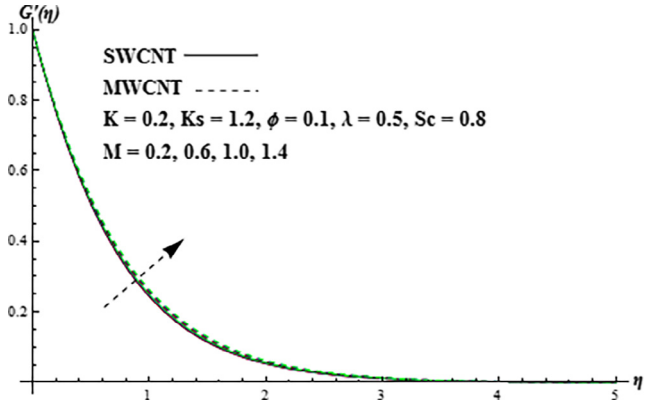

Fig. 6. M variation for G'.

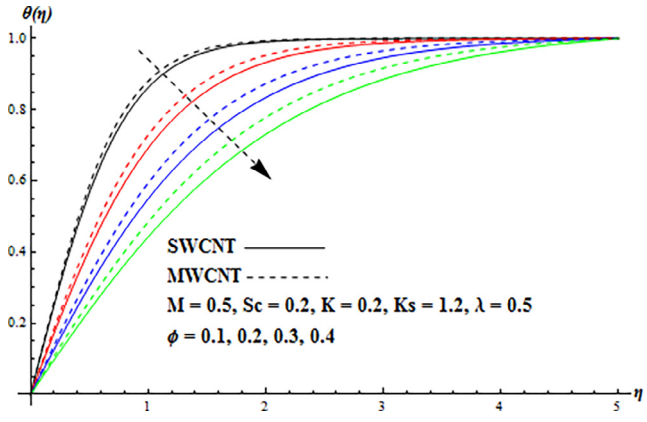

Fig. 7. ϕ variation for θ.

components of velocity. Clearly both velocity and corresponding boundary layer are enhanced for larger nanomaterial volume fraction ϕ. Furthermore the impact of multi-wall CNTs dominants over single-wall CNTs. Effect of porosity parameter λ on axial and transverse components of velocity is portrayed in Figs. (3) and (4). Here velocity decreases for larger porosity parameter λ. In fact the permeability of porous medium decreases for larger porosity parameter which leads to reduction of fluid velocity. Also effect of single-wall CNTs is more than multi-wall CNTs. Figs. (5) and (6) show outcome of melting parameter M on axial and transverse components of velocity. Here velocity profiles increase for larger melting parameter M in cases of both single and multi-wall CNTs. Influence of nanomaterial volume fraction ϕ on temperature is presented in Fig. 7. Clearly fluid temperature reduces while corresponding thermal boundary layer enhances for larger nanomaterial volume fraction ϕ. Fig. 8 shows influence of porosity parameter λ on temperature distribution. It is examined that for higher values of permeability parameter the fluid temperature decreases. In Fig. 9 analysis of melting parameter M on temperature is sketched. Temperature reduces for higher melting parameter M. In fact enlargement in melting parameter corresponds to convective flow of

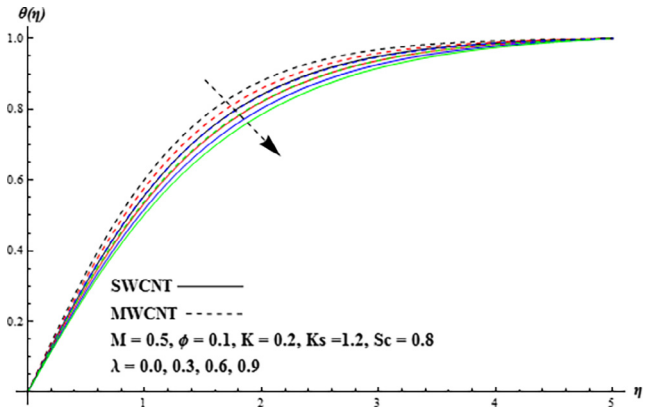

Fig. 8. λ variation for θ.

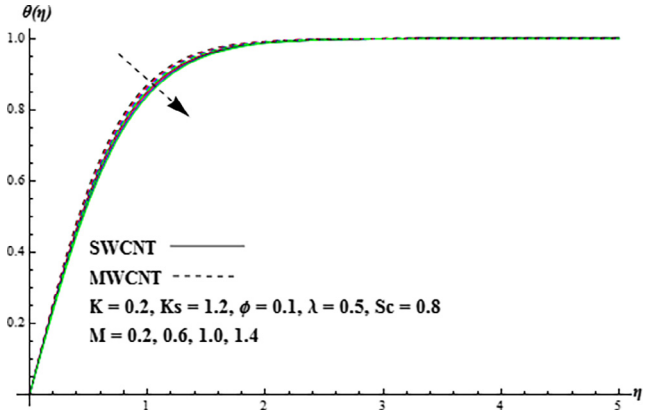

Fig. 9. M variation for θ.

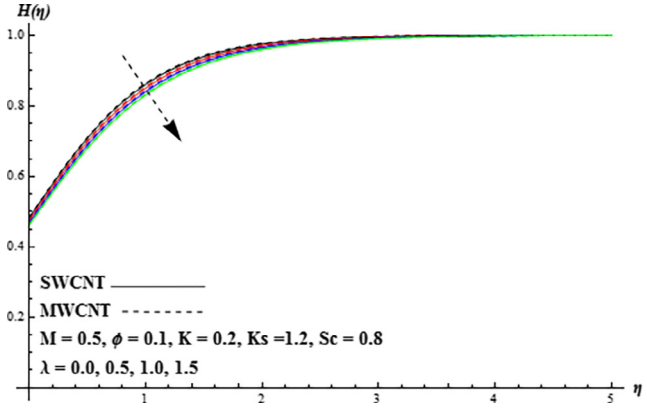

Fig. 10. λ variation for H.

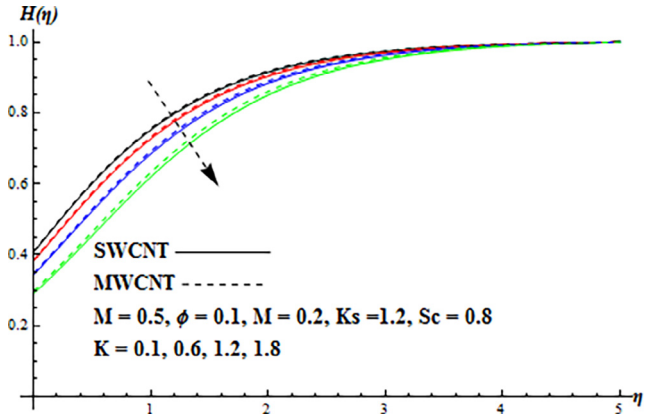

Fig. 11. K^* variation for H.

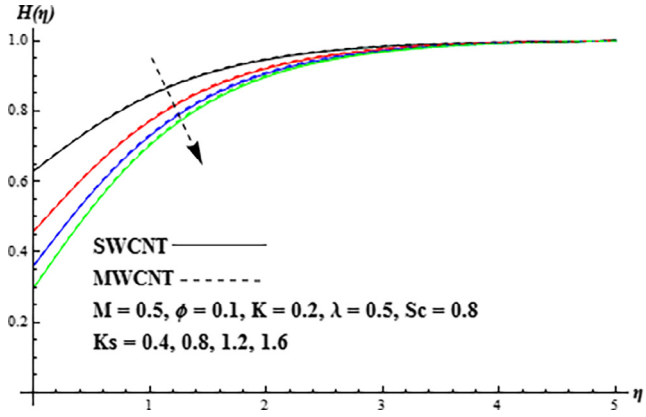

Fig. 12. Ks variation for H.

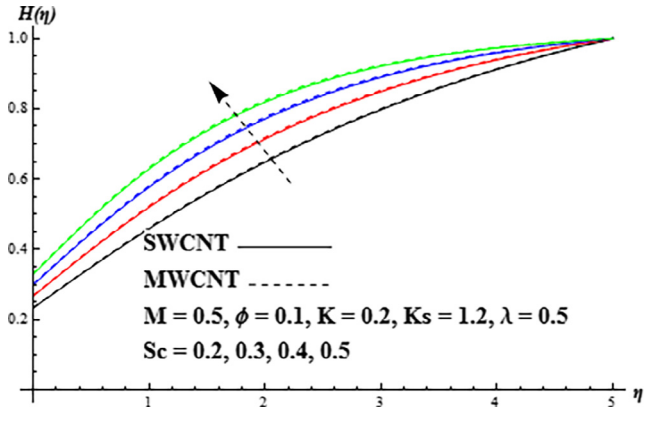

Fig. 13. Sc variation for H.

heated fluid to the melting surface. Influence of porosity parameter λ on concentration is depicted in Fig. 10. The concentration decreases for larger λ. Fig. 11 shows the effect of strength of homogenous reaction parameter K^* on the concentration. There is decrease in concentration for larger K^* while opposite behavior is inspected for boundary layer. Also the impact of single-wall CNTs dominants over multi-wall CNTs. Effect of strength of heterogenous reaction parameter K_s on concentration is sketched in Fig. 12. The result for K_s on concentration and associated boundary layer are similar to of K^*. Fig. 13. is depicted for the impact of Sc on concentration. It is inspected that concentration enhances while the corresponding solutal boundary layer decreases for larger Sc. The ratio of momentum diffusivity to mass diffusivity is called Schmidt number. Thus by increasing Schmidt number, mass diffusion

Table 1
Numerical values of specific heat, density and thermal conductivity.

Physical properties	Nanotubes		Base fluid
	SWCNT	MWCNT	Water
$c_p(J/kgK)$	425	796	4179
$\rho(kg/m^3)$	2600	1600	997
$k(W/mK)$	6600	3000	0.613

Table 2
Evaluation of coefficient of skin friction and Nusselt number under influential variables in both single and multi-wall CNTs cases when $K^* = 0.2, K_s = 1.2$ and $Sc = 0.8$.

ϕ	M	λ	*SWCNT* $c_f\sqrt{\mathrm{Re}_x}$	*MWCNT* $c_f\sqrt{\mathrm{Re}_x}$	*SWCNT* $c_f\sqrt{\mathrm{Re}_y}$	*MWCNT* $c_f\sqrt{\mathrm{Re}_y}$	*SWCNT* $\frac{Nu}{\sqrt{\mathrm{Re}_x}}$	*MWCNT* $\frac{Nu}{\sqrt{\mathrm{Re}_x}}$
0.1	0.5	0.5	−1.68714	−1.63180	−1.68720	−1.63187	−3.63323	−3.55854
0.2			−2.15488	−2.03959	−2.15500	−2.03976	−4.44146	−4.41693
0.3			−2.80679	−2.87050	−2.87050	−2.62161	−5.03448	−5.06319
0.1	0.2	0.5	−2.15488	−1.64363	−1.67920	−1.64371	−3.69830	−3.63775
	0.6		−1.69066	−1.62798	−1.68372	−1.63806	−3.61215	−3.53305
	1.0		−1.67020	−1.61331	−1.69432	−1.61339	−3.53067	−.43530
0.1	0.5	0.0	−1.42409	−1.35847	−1.42411	−1.35849	−3.75571	−3.67827
		0.5	−1.68714	−1.63180	−1.68720	−1.63187	−3.63323	−3.55854
		1.0	−1.91740	−1.86883	−1.91742	−1.86885	−3.52595	−3.45443

decreases which is responsible for an enhancement of concentration.Table 1 illustrates specific heat, density and thermal conductivity of the carbon nanotubes and water while Table 2 is made for the numerical data of skin friction coefficient and Nusselt number. The skin friction coefficient is more for lager nanomaterial volume friction ϕ. However it decreases for melting parameter M and porosity parameter λ in both cases of SWCNTs and MWCNTs. Effects of SWCNTs dominant over MWCNTs. Nusselt number shows increasing behavior for larger nanomaterial volume fraction while it has opposite behavior for melting M and porosity λ parameters. Effect of SWCNTs on Nusselt number is more when compared with MWCNTs.

Concluding remarks

In the present work we have discussed melting heat transfer in the flow of CNTs. The outcomes are listed as follows:

- Velocity distributions (axial and transverse components of velocity) shows increasing behavior for larger nanomaterial volume fraction ϕ. However such velocities have opposite behavior for porosity parameter λ and melting parameter M. Impact of multi-wall CNTs dominants over single-wall CNTs.
- Temperature is smaller for larger nanomaterial volume fraction ϕ, melting parameter M and porosity parameter λ. Furthermore single-wall CNTs are more efficient than multi-wall CNTs.
- Larger strength of homogenous reaction parameter K^* and strength of heterogenous reaction parameter K_s cause reduction of concentration. However it enhances for higher values of Schmidt number Sc.
- Larger nanomaterial volume fraction ϕ cause enlargement in the coefficient of skin friction for both single and multi-wall CNTs cases. Also skin friction coefficient reduces for larger melting M and porosity λ parameters.
- Heat transfer rate or cooling process can be increased by utilizing smaller porosity parameter λ and melting parameter M. However it reduces for larger nanomaterial volume fraction ϕ. It is seen that SWCNT case is more effective than MWCNT.

References

[1] Choi SUS. Enhancing thermal conductivity of fluids with nanoparticles, In: Siginer DA, Wang HP. editor. Development and Application of non-Newtonian flows. FED-vol. 231/MD 66, New York: ASM; 1995.p. 99–105.
[2] Elias MM, Miqdad M, Mahbubul IM, Saidur R, Kamalisarvestani M, Sohel MR, et al. Effect of nanoparticle shape on the heat transfer and thermodynamic performance of a shell and tube heat exchanger. Int Commun Heat Mass Transf 2013;44:93–9.
[3] Volder MFLD, Tawfick SH, Baughman RH, Hart AJ. Carbon nanotubes: present and future commercial applications. Science 2013;339:535–9.
[4] Waqas M, Hayat T, Shehzad SA, Alsaedi A. Transport of magnetohydrodynamic nanomaterial in a stratified medium considering gyrotactic microorganisms. Physica B 2018;529:33–40.
[5] Nayak RK, Bhattacharyya S, Pop I. Numerical study on mixed convection and entropy generation of Cu-water nanofluid in a differentially heated skewed enclosure. Int J Heat Mass Transf 2015;85:620–34.
[6] Hayat T, Farooq M, Alsaedi A. Stagnation point flow of carbon nantubes over a stretching cylinder with slip conditions. Open Phys 2015;13:188–97.
[7] Shiekholeslami M, Ellahi R. Three dimensional mesoscopic simulation of magnetic field effect on natural convection of nanofluid. Int J Heat Mass Transf 2015;89:799–808.
[8] Hayat T, Waqas M, Shehzad SA, Alsaedi A. A model of solar radiation and Joule heating in magnetohydrodynamic (MHD) convective flow of thixotropic nanofluid. J Mol Liq 2016;215:704–10.
[9] Waqas M, Khan MI, Hayat T, Alsaedi A. Numerical simulation for magneto Carreau nanofluid model with thermal radiation: a revised model. Comput Methods Appl Mech Eng 2017;324:640–53.
[10] Roberts L. On the melting of a semi infinite body of ice placed in a hot stream of air. J Fluid Mech 1958;4:505–28.
[11] Hayat T, Farooq M, Alsaedi A. Melting heat transfer in the stagnation point flow of Maxwell fluid with double-diffusive convection. Int J Numer Methods Heat Fluid Flow 2014;24:760–74.
[12] Das K. Radiation and melting effects on MHD boundary layer flow over a moving surface. Ain Shams Eng J 2014;5:1207–14.
[13] Yacob NA, Ishak A, Pop I. Melting heat transfer in boundary layer stagnation-point flow towards a stretching/shrinking sheet in a micropolar fluid. Comput Fluids 2011;47:16–21.
[14] Bachok N, Ishak A, Pop I. Melting heat transfer in boundary layer stagnation-point flow towards a stretching/ shrinking sheet. 4079. Phys Lett A 2010;374:4075.
[15] Ho CJ, Gao JY. An experimental study on melting heat transfer of paraffin dispersed with Al_2O_3 nanoparticles in a vertical enclosure. Int J Heat Mass Transf 2013;62:2–8.
[16] Waqas M, Farooq M, Khan MI, Alsaedi A, Hayat T, Yasmeen T. Magnetohydrodynamic (MHD) mixed convection flow of micropolar liquid due to nonlinear stretched sheet with convective condition. Int J Heat Mass Transf 2016;102:766–72.
[17] Waqas M, Hayat T, Farooq M, Shehzad SA, Alsaedi A. Cattaneo-Christov heat flux model for flow of variable thermal conductivity generalized Burgers fluid. J Mol Liq 2016;220:642–8.
[18] Hayat T, Mustafa M, Asghar S. Unsteady flow with heat and mass transfer of a third grade fluid over a stretching surface in the presence of chemical reaction. Nonlinear Anal Real World Appl 2010;11:3186–97.
[19] Hayat T, Waqas M, Khan MI, Alsaedi A. Analysis of thixotropic nanomaterial in a doubly stratified medium considering magnetic field effects. Int J Heat Mass Transf 2016;102:1123–9.
[20] Hayat T, Shehzad SA, Qasim M, Obaidat S. Radiative flow of Jeffery fluid in a porous medium with power law heat flux and heat source. Nucl Eng. Des 2012;243:15–9.
[21] Khan M, Maqbool K, Hayat T. Influence of Hall current on the flows of a generalized Oldroyd-B fluid in a porous space. Acta Mech 2006;184:1–13.
[22] Hayat T, Imtiaz M, Alsaedi A, Kutbi MA. MHD three-dimensional flow of nanofluid with velocity slip and nonlinear thermal radiation. J Magn Magn Mater 2015;396:31–7.
[23] Hayat T, Shehzad SA, Alsaedi A. Soret and Dufour effects on magnetohydrodynamic (MHD) flow of Casson fluid. Appl Math Mech Engl Ed 2012;33:1301–12.
[24] Merkin JH. A model for isothermal homogenous-heterogenous reactions in boundary-layer flow. Math Comput Model 1996;24:125–36.
[25] Hayat T, Farooq M, Alsaedi A. Homogenous-heterogenous reactions in the stagnation point flow of carbon nanotubes with Newtonian heating. AIP Adv 2015;5:027130.
[26] Kameswarn PK, Shaw S, Sibanda P, Murthy PVSN. Homogenous-heterogenous reactions in a nanofluid flow due to a porous stretching sheet. Int J Heat Mass Transf 2013;57:465–72.
[27] Shaw S, Kameswaran P, Sibanda P. Homogenous-heterogenous reactions in micropolar fluid flow from a permeable stretching or shrinking sheet in a porous medium. Boundary Value Probl 2013;2013:77.
[28] Bachok N, Ishak A, Pop I. On the stagnation-point flow towards a stretching sheet with homogeneous-heterogeneous reactions effects. Commun Nonlinear Sci Numer Simul 2011;16:4296–302.

[29] Song X, Schmidt LD, Aris R. Steady states and oscillations in homogeneous—heterogeneous reaction systems. Chem Eng Sci 1991;46:1203–15.
[30] Qayyum S, Hayat T, Alsaedi A. Chemical reaction and heat generation/absorption aspects in MHD nonlinear convective flow of third grade nanofluid over a nonlinear stretching sheet with variable thickness. Res Phys 2017;7:2752–61.
[31] Hayat T, Ayub T, Muhammad T, Alsaedi A. Three-dimensional flow with Cattaneo-Christov double diffusion and homogeneous-heterogeneous reactions. Res Phys 2017;7:2812–20.
[32] Tanveer A, Hayat T, Alsaedi A, Ahmad B. Mixed convective peristaltic flow of Sisko fluid in curved channel with homogeneous-heterogeneous reaction effects. J Mol Liq 2017;233:131–8.
[33] Hayat T, Bibi A, Yasmin H, Ahmad B. Simultaneous effects of Hall current and homogeneous/heterogeneous reactions on peristalsis. J Taiwan Inst Chem Eng 2016;58:28–38.
[34] Khan MI, Hayat T, Khan MI, Alsaedi A. A modified homogeneous-heterogeneous reactions for MHD stagnation flow with viscous dissipation and Joule heating. Int J Heat Mass Transf 2017;113:310–7.
[35] Hayat T, Hussain Z, Muhammad T, Alsaedi A. Effects of homogeneous and heterogeneous reactions in flow of nanofluids over a nonlinear stretching surface with variable surface thickness. J Mol Liq 2016;221:1121–7.
[36] Hayat T, Khan MI, Farooq M, Yasmeen T, Alsaedi A. Stagnation point flow with Cattaneo-Christov heat flux and homogeneous-heterogeneous reactions. J Mol Liq 2016;220:49–55.
[37] Imtiaz M, Hayat T, Alsaedi A, Hobiny A. Homogeneous-heterogeneous reactions in MHD flow due to an unsteady curved stretching surface. J Mol Liq 2016;221:245–53.
[38] Hayat T, Imtiaz M, Alsaedi A, Almezal S. On Cattaneo-Christov heat flux in MHD flow of Oldroyd-B fluid with homogeneous–heterogeneous reactions. J Magn Magn Mater 2016;401:296–303.
[39] Hayat T, Khan MI, Farooq M, Yasmeen T, Alsaedi A. Stagnation point flow with Cattaneo-Christov heat flux and homogeneous-heterogeneous reactions. J Mol Liq 2016;220:49–55.
[40] Xue Q. Model for thermal conductivity of carbon nanotube based composites. Phys B Condens Matter 2005;368:302–7.
[41] Ali N, Sajid M, Abbas Z, Javed T. Non-Newtonian fluid flow induced by peristaltic waves in a curved channel. Eur J Mech B/Fluids 2010;29:387–94.
[42] Mustafa M, Hina S, Hayat T, Alsaedi A. Influence of wall properties on the peristaltic flow of a nanofluid: analytic and numerical solutions. Int J Heat Mass Transf 2012;55:4871–7.